Wide Range Vacuum Pumps for the SAM Instrument on the MSL Curiosity Rover

Paul Sorensen*, Robert Kline-Schoder* and Rodger Farley**

Abstract

Creare Incorporated and NASA Goddard Space Flight Center developed and space qualified two wide range pumps (WRPs) that were included in the Sample Analysis at Mars (SAM) instrument [1]. This instrument was subsequently integrated into the Mars Science Laboratory (MSL) "Curiosity Rover," launched aboard an Atlas V rocket in 2011, and landed on August 6, 2012, in the Gale Crater on Mars. The pumps have now operated for more than 18 months in the Gale Crater and have been evacuating the key components of the SAM instrument: a quadrupole mass spectrometer, a tunable laser spectrometer, and six gas chromatograph columns. In this paper, we describe the main design challenges and the ways in which they were solved. This includes the custom design of a miniaturized, high-speed motor to drive the turbo drag pump rotor, analysis of rotor dynamics for super critical operation, and bearing/lubricant design/selection.

Introduction

Approximately 15 years ago, the Jet Propulsion Laboratory started an initiative to fund the development of a miniaturized vacuum system. JPL saw a need for small vacuum systems to support astrobiological science missions, including mass spectrometers and gas chromatographs. At the time, mass spectrometers and other instruments for astrobiology were being reduced in size, mass, and power. However, the bulk of the accompanying vacuum system had come to dominate the overall system design, especially since commercial vacuum systems were not designed with the constraints of space missions in mind. For astrobiological science missions such as MSL, the main requirements are the highest vacuum level and longest life in the smallest possible package with the least amount of power consumption. These are requirements not unlike what is required for terrestrial applications of portable mass spectrometers. This paper will present miniaturized pumping system design and test data and will discuss continuing efforts, supported by Goddard Space Flight Center (GSFC), to demonstrate long life time with repeated start-stop cycles.

Miniature Vacuum Pump Background

In order to achieve high vacuum levels, only a few pumping technologies are available (turbomolecular-, cryogenic-, or diffusion-pumps). Considering size and power limitations, the choices are further restricted so that the only viable technology for long term operation is a turbomolecular pump. In a turbomolecular pump, the rotor and stator blades push gas molecules from low to high pressure. In order to achieve high compression ratios on each turbo stage, the pump rotor tip speed needs to be comparable to the most probable molecular speed of the gas being pumped. This means that when the size of the rotor decreases to reduce pump size and mass, the rotor speed needs to increase in proportion. Also, as pump size decreases, the pumping speed is reduced, which necessitates tighter clearances between the moving parts of the pumps in order to control leakage back flow. Both the higher speed and the tighter clearance affect higher demand on pump parts fabrication and assembly. For astrobiological science, and Mars missions in particular, a turbomolecular pump (TMP) is coupled with a molecular drag pump (MDP) on the same shaft driven by the same electric motor drive. The molecular drag pump exhausts directly to

* Creale Incorporated, Hanover, NH

** NASA Goddard Space Flight Center, Greenbelt, MD

Proceedings of the 42nd Aerospace Mechanisms Symposium, NASA Goddard Space Flight Center, May 14-16, 2014

the Martian atmosphere at pressure 10 Torr or greater. Similar demands for high precision manufacture and assembly of the molecular drag pump exist as for the turbo-molecular pump.

In collaboration with GSFC, Creare has been developing and demonstrating the technologies required to design and build miniature high vacuum pumps. In particular, we have designed and built two of the smallest available high vacuum pumps that have the following pumping characteristics: a compression ratio for air that is greater than 10e8; a pumping speed of about 5 L/sec; 10-W power consumption for an exhaust pressure of 10 Torr; and operation over a very wide range of temperatures (from -40°C to 65°C). The smallest of these pumps (Figure 1a) has a mass of 130 g, a diameter of 3.3 cm (1.3 in), and an overall length of 5.8 cm (2.3 in) (i.e., the size of a C-cell battery). The slightly larger pump (Figure 1b) has a mass of 500 g, a diameter of 5.1 cm (2.0 in), and an overall length of 11.7 cm (4.6 in) (i.e., the size of a soda can). The larger version was space qualified for use on the Mars Science Laboratory (MSL) Sample Analysis at Mars (SAM) instrument that was launched in 2011 and is currently being used operationally on Mars. The smaller version was tested to TRL 6 in the laboratory for potential use on ExoMars, a reformulated Mars mission, or other astrobiological missions.

(a) **(b)**

Figure 1. (a) Smallest Turbomolecular/Molecular Drag Pump. (b) Space-Qualified Turbomolecular/Molecular Drag Pump That is Part of the SAM Instrument on MSL.

Vacuum Pump Fabrication Challenges

As described above, in order to greatly reduce the size and mass of a TMP/MDP, very high rotor speeds are required since the pump tip speed must remain constant as the pump diameter is decreased. In order to achieve the desired size and mass for space missions, the miniaturized pumps that we have developed require motor operation at 100,000 rpm (for the 5.1-cm-diameter pump) and 200,000 rpm (for the 3.3-cm-diameter pump). Table 1 summarizes the features enabled by miniaturization and those required for space qualification and the corresponding consequence and fabrication challenge. While the need for tight dimensional control, the selection of proper materials, and accommodating the consequences of thermal and structural interactions require careful engineering design, the most difficult challenge that we faced was the impact of very high speed operation of the motors on lifetime of the pumps. In particular, since the miniaturized pumps need to operate at such high speeds, the combined motor and rotor structural resonances are below the operating speed of the pump, which results in super-critical operation. This, combined with the need for relatively long-life under harsh operating conditions (i.e., many starts/stops) resulted in the key limitation that needed to be overcome during space qualification. In fact, TMP/MDPs designed for use on Earth are turned on once and rarely, if ever, turned off and on again, in order to avoid the wear-and-tear associated with starting and stopping the pumps. In addition, terrestrial TMP/MDPs are operated at sub-critical speeds.

Miniaturized TMP/MDP Design

The design of the miniaturized, space-qualified TMP/MDP is shown in Figure 2. Figure 2a provides an exploded view and Figure 2b provides a cross sectional view of the pump. This figure shows that the pump rotor is cantilevered over the pump motor and that the turbomolecular blades are on the outside of the pump rotor near the gas inlet and that the smooth molecular drag pump rotor begins on the outside of the pump rotor and continues on the inside of the pump rotor, making use of the bottom end of the pump stator and the outside of the pump motor for the molecular drag pump "grooves".

Table 1. Summary of Miniaturized Turbomolecular/Molecular Drag Pump Fabrication Challenges.

Feature	Consequence	Fabrication challenge
Lower pumping speed	Good internal leakage control	Tight dimensional control
Smaller dimensions	Small clearances in flow channels	Tight dimensional control
High speed	Super critical operation	Advanced balancing procedures
High speed, lightweight	Material structural limits	Use high strength alloys
Wide temperature range	Compatible material selection	Incorporate heater and heat rejection
Wide temperature swing	CTE mismatch	Careful thermal/structural design

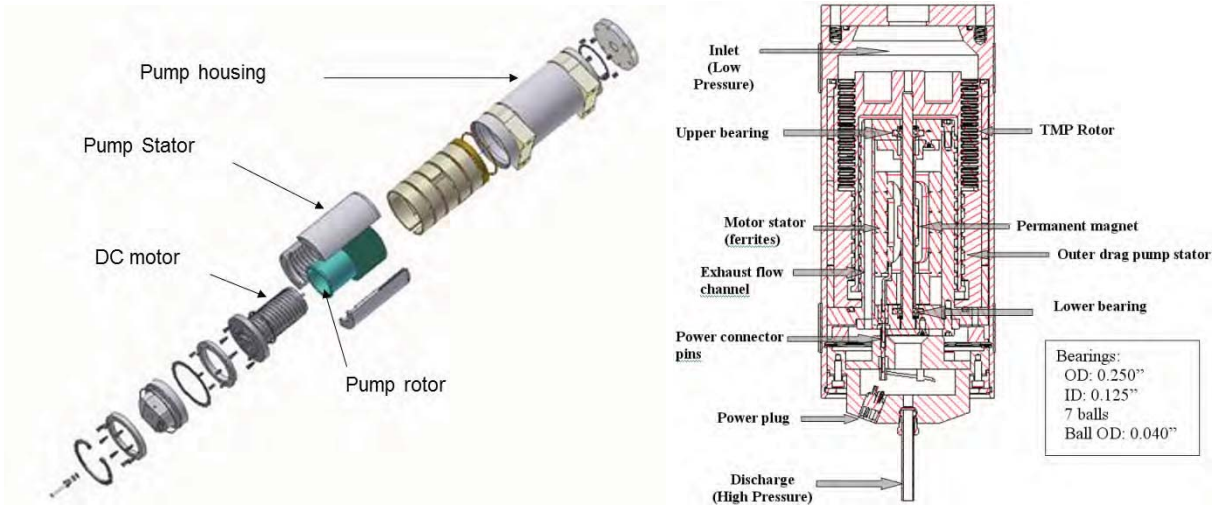

(a) **(b)**

Figure 2. (a) Exploded, Three-Dimensional View of Space-Qualified 100,000 rpm TMP/MDP (b) Cross Section of Space-Qualified 100,000 rpm TMP/MDP

Resonant Frequency Analysis Optimization

Analysis of the motor rotor/pump rotor combination (see Figure 3) show that the lowest natural frequency of the combined system is approximately 985 Hz (e.g. approximately 59,000 rpm) and that the mode shape is such that the pump rotor acts like a bell on the "stiff", tungsten-carbide shaft with the bearings providing the support points. In order to make the natural frequency of this mode as high as possible, we have designed the pump so that the bearings are as close as possible to each other given the other constraints of the motor design (namely the electro-magnetic requirements of the low-power, high-speed motor). In order to enable the pump motor to pass through this resonance, we have mounted the bearings in an elastomer, which provides both greater damping and lower stiffness as compared to hard-mounted bearings. While these properties enable super-critical operation, they also presented operational

temperature range challenges and necessitated the introduction of a heater on the pump to ensure that the elastomer was soft enough during startup to provide these important properties.

Lifetime Optimization

As described above, high-speed operation, super-critical operation, and the need for many start and stop cycles contributed to the need to optimize the lifetime of the pump to meet the mission requirements. In addition, since science considerations limited the choice of lubricant to non-hydrocarbon greases, the bearing-lubricant combination selection became the focus of an effort to optimize the pump lifetime. We used a combination of screening tests at room temperature with hardware that consisted of the pump motor and a pump rotor simulator (i.e., "Life Test Simulators") as well as complete pumps that were tested over the complete operational temperature range of the mission.

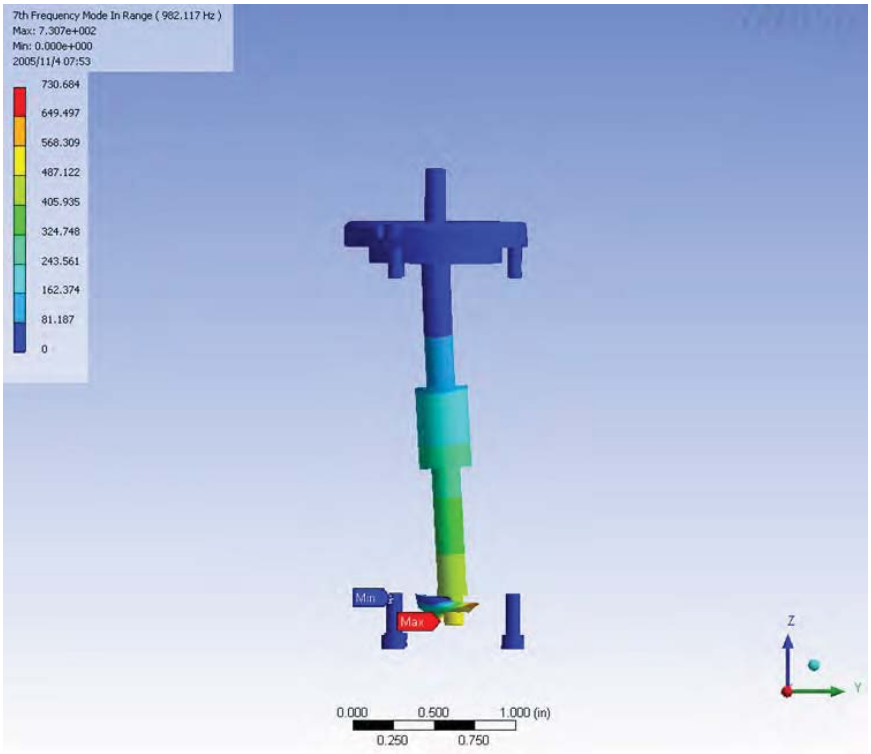

Figure 3. Fundamental Structural Resonance Mode Shape From Finite Element Analysis

A summary of the test configurations and the results of the life testing using the Life Test Simulators are shown in Table 2. Based on the results of similar previous tests and input from bearing and lubricant experts, we focused our testing on two retainer materials and various pre-load values. We focused our testing on these variations because results of our previous testing indicated that cracking or wear of the retainers was the primary, life-limiting, failure mechanism. In addition, based on results of our testing, the bearing manufacturer revised the design of their standard Meldin retainer to provide additional a larger cross section of material. Finally, we considered the effect of pre-load since the overall design required that the bearings be pre-loaded and past experience showing a significant effect of pre-load on bearing and lubricant life. The results show that the Vespel retainers, which are strong, but which do not absorb much lubricant, can be made to last twice the desired lifetime specification. However, the performance of this material and the lubricant is strongly related to the pre-load. The Meldin retainer material, being porous, stores lubricant and can therefore achieve a longer life time – up to and beyond three times the desired lifetime specification.

Table 2. Summary of Life Test Simulator Configurations and Results

Test Unit #	Retainer Material	Pre-Load (N)/(lb)	Lifetime (hr)	Fraction of Spec
3	Vespel	2.7 / 0.6	801	1.59
4	Vespel	1.8 / 0.4	1027	2.04
5	Vespel	4.0 / 0.9	575	1.09
6	Meldin (original)	2.7 / 0.6	1160	2.21
7	Meldin (revised)	1.8 / 0.4	1736	3.31
8	Meldin (revised)	2.7 / 0.6	1690	3.22
9	Meldin (revised)	2.7 / 0.6	1343	2.56

Vacuum Pump Measured Performance

The Martian atmosphere, though much lower pressure than Earth (e.g., approximately 10 torr of mostly CO_2), is still much too dense for mass spectrometers to work. The SAM instrument requires two vacuum pumps that are able to exhaust directly to the Martian atmosphere and much achieve high vacuum levels. In order to meet the high compression ratio, we developed a miniaturized hybrid turbomolecular and molecular drag pump with unique features. The pump is shown in Figure 4 after installation in the SAM instrument. The pump is less than half the size of the smallest turbo drag vacuum pump available commercially and consumes only one-tenth of the power. As a consequence of the smaller size, this turbo drag spins at 100,000 rpm.

Figure 4. Wide Range Pump Installed in SAM Instrument

During the course of the pump development, we measured the ultimate pressure and flow rate of the pump design. The ultimate pressure test measures high vacuum pressure on the upstream side of the WRP while maintaining a given exhaust pressure on the downstream side of the WRP and the flow is only that due to outgassing in the test chamber (assumed to be very small). The tests are conducted first with the pump purged with CO_2 and CO_2 on the exhaust side and subsequently with a thorough Helium purge and Helium on the exhaust side. The pressure measurements are conducted in an environmental chamber with the chamber temperature set at 22 °C, +50 °C and -40 °C respectively.

The pump was started at room temperature, brought up to full speed, 100,000 rpm, and maintained at this speed during temperature cycling. The pump was initially brought up to +50 °C to allow as much of the entrained gas in the high vacuum chamber to outgas as possible. We did observe a steady decline of the high vacuum pressure throughout the test as the chamber was cleaned of outgassing material. The chamber had been rough pumped for several days prior to testing, but even so improved high vacuum performance will probably be possible with a more thorough bake out and cleaning with a turbo pump. So, the results reported here can be seen as conservative and provide a lower limit on vacuum pump

compression ratio. At each of the three temperatures, we recorded the steady-state high vacuum pressure, the pump foreline pressure, the DC voltage and current into the motor controller, and the pump housing temperature. The high vacuum pressure was collected with a Bayard-Albert (BA) tube. A correction factor was applied to the indicated pressure to account for the difference in gas performance of the BA tube. The foreline pressure is measured with a Convectron gauge and properly corrected for the difference in gas convection properties.

The measured ultimate pressure and resulting compression ratio for CO_2 as a function of foreline pressure are given in Figure 5. We see that the pump maintains a virtually constant high vacuum pressure, but that this pressure is highly dependent on the temperature. The pumping ability of the turbo molecular pump is expected to be reduced with increased mean molecular speed. However, this only accounts for a very minor amount (<10%) of change in no-flow pressure. Barring any increase in leakage across the pump, we expect the main reason for increased ultimate pressure at high temperature to be due to increased outgassing in the vacuum chamber, which is also supported by the fact that the pressure at similar operating conditions kept dropping during the test as the chamber was baked out. We see that the compression ratio at Mars operating conditions exceeds 5e6 at high temperature and is close to 10e8 at low temperature.

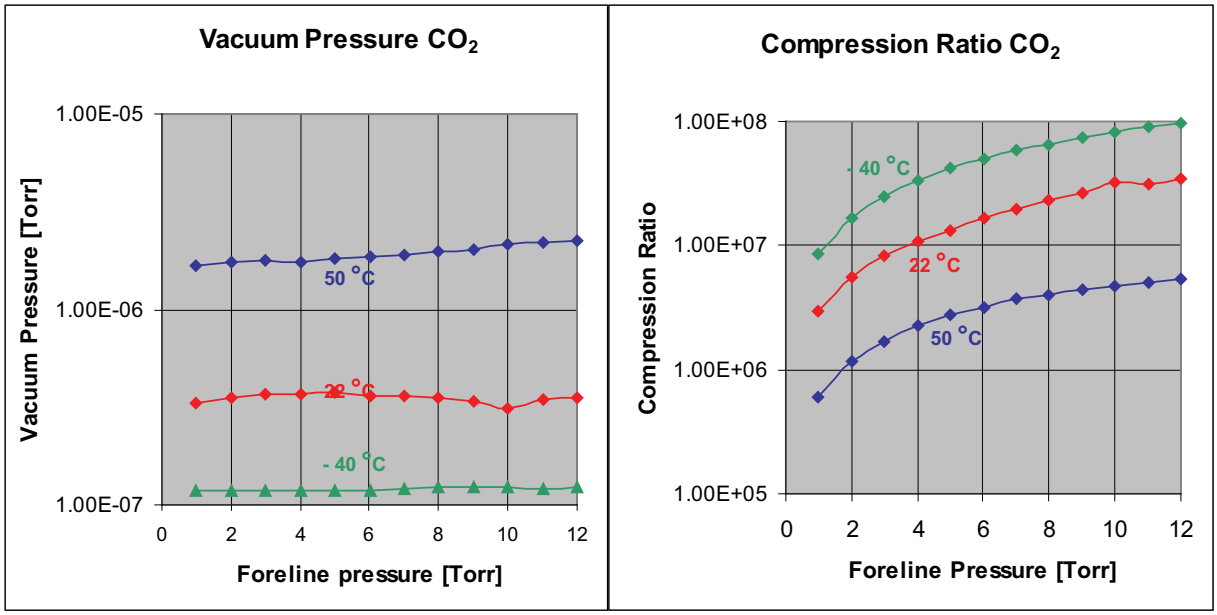

Figure 5. Ultimate Pressure and Compression Ratio Pumping CO_2

The flow test measures the pumping speed of the WRP while maintaining an exhaust pressure on the downstream side of the WRP similar to Martian conditions of 12 Torr. The tests were conducted in three configurations: (1) the pump purged with CO_2 and CO_2 on the exhaust side; (2) a thorough Helium purge and CO_2 on the exhaust side; and (3) N_2 on both high vacuum and exhaust side of the pump. During the tests CO_2, Helium, or N_2 is bled into the high vacuum chamber through an orifice and the pressure drop across the orifice is used to determine the flow rate and thereby the pumping speed. The measurements are conducted in an environmental chamber with the chamber temperature set at +20°C, +50°C and -40°C respectively.

The pump was started at room temperature, brought up to full speed, 100,000 rpm, and maintained at this speed during temperature cycling. The chamber was initially brought up to +50 °C to allow as much of the entrained gas in the high vacuum chamber to outgas as possible. We did observe a steady decline of the high vacuum pressure throughout the test as the chamber was cleaned of outgassing material. The chamber had been rough pumped for several days prior to testing, but even so improved high vacuum performance will probably be possible with a more thorough bake out and cleaning with a turbo pump.

The pumping speed measurements will be affected by the outgassing rates, in particular at low temperatures where it will underestimate the flow rate. The pumping speed is derived by bleeding the gas through a short circular duct of known dimensions into the high vacuum chamber. Assuming that the gas flow through the duct is much larger than outgassing rates, the duct flow rates will equal pumping speed. The duct flow rate can be determined from measurements of gas pressure on either side of the duct.

At each of the three temperatures, we recorded the steady-state high vacuum pressure, the gas leak pressure upstream from the metering duct, the pump foreline pressure, the DC voltage and current into the motor controller, and the pump housing temperature. We also measured the temperature of the chamber wall upstream of the orifice and used this temperature as a measure of the temperature of the gas flowing through the orifice. Since this chamber is large both in length and diameter relative to the gas mean free path, and since the gas flow through this chamber is very slow, the gas has ample time to reach thermal equilibrium with the chamber walls. If the real gas temperature is actually different, the duct conductance will be wrong but we estimate that this error will be less than a few percent. The high vacuum pressure was measured with a BA tube. A correction factor was applied to the indicated pressure to account for the difference in gas performance of the BA tube. The foreline pressure is measured with a Convectron gauge and properly corrected for the difference in gas convection properties. The bleed pressure was measured with a calibrated Pirani gauge, and corrected for the difference in gas conductivity of Helium, CO_2, and N_2. The main uncertainty in the flow measurement is due to the error in the BA tube measurement. This will directly affect the pumping speed measurement. We estimate the total relative error on the pumping speed to be 20-25%.

We measured the pumping speed by adjusting the setting of a leak valve on the upstream side of the metering duct. We covered flow rates through the duct from zero to a value where the pressure upstream of the metering duct (the leak pressure) gave a mean free path of the gas molecules ten times longer than the duct diameter. This ensures that the duct conductance can be treated as purely molecular flow far from transitioning to continuum flow. The measured pumping speed is shown in Figure 6 for the three gasses and three gas temperatures spanning the temperature extremes for the WRP operation. We see that the pumping speed at high vacuum pressure (i.e., small differential pressure across the orifice) reaches a constant level of approximately 6 L/sec. This level is consistent with model values for the turbo-molecular stage at zero differential pressure across the turbo molecular stages. When the high vacuum pressure (i.e. inlet to the pump) is lowered the pumping speed decreases, since the probability of a molecule hitting the pump inlet goes down to the point where as many molecules enter the pump inlet as exit it.

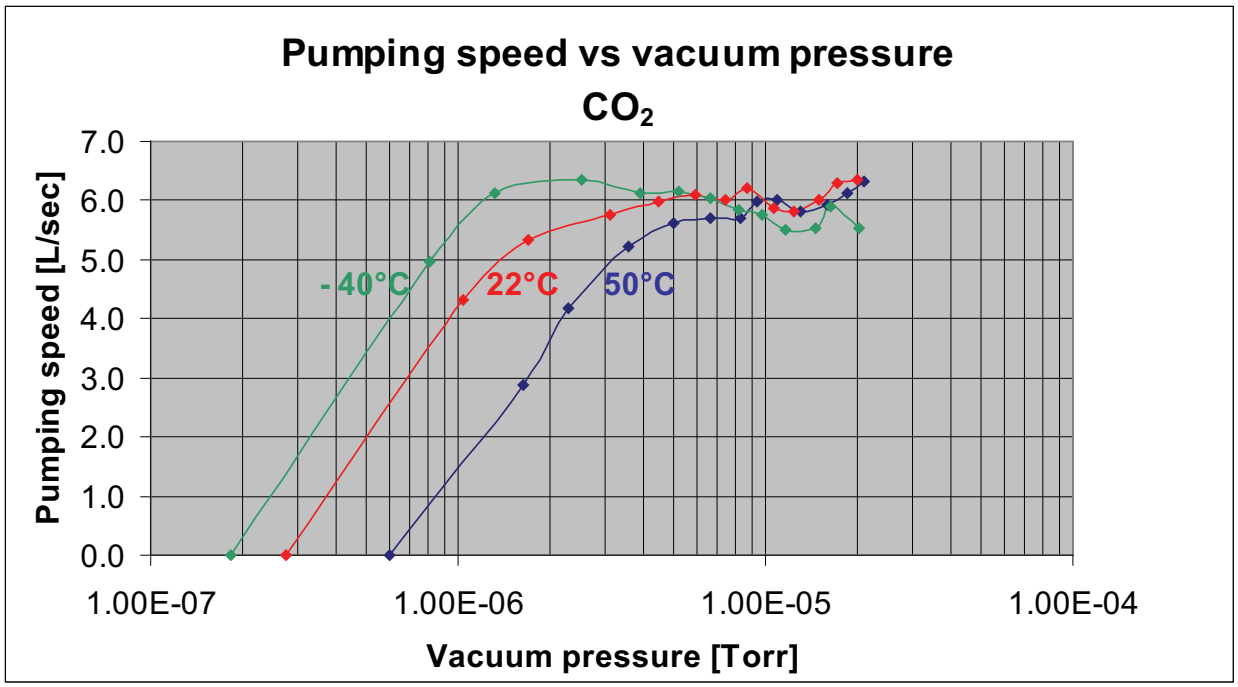

Figure 6. WRP Pumping Speed When Pumping CO_2 With Exhaust of CO_2 at 12 torr

The pumping speed is clearly affected by temperature, the pump being less efficient at higher temperature. The main difference between high and low temperatures is believed to be the level of outgassing from the vacuum chamber wall. At higher temperatures, the outgassing will increase substantially, thereby adding leak flow to the orifice flow that the WRP must pump. The pumping speed at high temperatures will therefore be artificially low. By proper bake out procedures we believe that the outgassing leak rate may be lowered substantially, which will result in increased measured pumping speed of the WRP.

Conclusions

In this paper, we described the main design challenges of designing and developing a space-qualified, miniature turbomolecular/molecular drag pump and the ways in which they were solved. This included a discussion of the custom design of a miniaturized high speed motor to drive the turbo drag pump rotor, analysis of rotor dynamics for super critical operation, and bearing/lubricant design and selection. Measured performance and lifetime data proved that the pump design achieved the mission specifications and current operation on Mars proves that the pump is meeting mission requirements.

References

1. Mahaffy, P.R., et al. “The Sample Analysis at Mars Investigation and Instrument Suite.” Space Science Reviews, September 2012, Volume 170, Issue 1-4, pp 401-478.